Environmental Technology & Innovation 19 (2020) 100847

Contents lists available at ScienceDirect

Environmental Technology & Innovation

journal homepage: www.elsevier.com/locate/eti

# Engineered tea-waste biochar for the removal of caffeine, a model compound in pharmaceuticals and personal care products (PPCPs), from aqueous media

S. Keerthanan [a], Amit Bhatnagar [b], Kushani Mahatantila [c], Chamila Jayasinghe [d], Yong Sik Ok [e,*], Meththika Vithanage [a,*]

[a] Ecosphere Resilience Research Center, Faculty of Applied Sciences, University of Sri Jayewardenepura, Nugegoda 10250, Sri Lanka
[b] Department of Environmental and Biological Sciences, University of Eastern Finland, P.O. Box 1627, FI-70211 Kuopio, Finland
[c] Chemical and Microbiological Laboratory, Industrial Technology Institute, Colombo 7, Sri Lanka
[d] Department of Food Science and Technology, Faculty of Livestock, Fisheries and Nutrition, Wayamba University of Sri Lanka. Makandura, Gonawila (NWP), Sri Lanka
[e] Korea Biochar Research Center, O-Jeong Eco-Resilience Institute (OJERI) & Division of Environmental Science and Ecological Engineering, Korea University, Seoul 02841, South Korea

ARTICLE INFO

*Article history:*
Received 21 December 2019
Received in revised form 26 April 2020
Accepted 26 April 2020
Available online 28 April 2020

*Keywords:*
Caffeine
Tea waste
Water treatment
Micropollutant
Stimulant drug
Engineered biochar

ABSTRACT

This study aimed to synthesize engineered tea-waste biochar, pyrolyzed at 700 °C using steam activation (TWBC-SA) for caffeine (CFN) removal from aqueous media. The morphological features and available functional groups on the surface of biochar were characterized using scanning electron microscopy (SEM), Fourier-transform infrared spectroscopy (FTIR), and X-ray photoelectron spectroscopy (XPS). Adsorption batch experiments were carried out at various pH values (3–10), contact time (up to 24 h), and initial concentration of CFN (10–300 mg $L^{-1}$) using 1 g $L^{-1}$ of TWBC-SA at 25 °C. SEM images showed the distribution of well-developed pores on the surface of biochar. FTIR spectra revealed that the surface of TWBC-SA provided extra aromatic character, which was further confirmed by XPS analysis. pH-adsorption edge data showed a maximum adsorption capacity of 15.4 mg $g^{-1}$at pH 3.5. The experimental data were best-fitted to the non-linear Elovich kinetic model, demonstrating the contribution of chemical forces for adsorption of CFN onto the heterogeneous surface of TWBC-SA (initial rate of adsorption = 55.6 mg $g^{-1}min^{-1}$). Non-linear forms of Freundlich and Temkin isotherm models were fitted with the experimental data, describing favorability of chemical interactions between CFN and TWBC-SA. Finally, it is demonstrated that the adsorption of CFN by TWBC-SA is mainly governed by the chemisorption mechanism via electrostatic interactions and nucleophilic attraction. Thus, the engineered steam-activated tea-waste biochar has a high potential for adsorbing CFN from water.



## 1. Introduction

With the improvement in the quality of life, natural water bodies are ultimately influenced by a variety of micropollutants, including hormones, pharmaceuticals, and personal care products (PPCPs), and endocrine-disrupting compounds

* Corresponding authors.
*E-mail addresses:* yongsikok@korea.ac.kr (Y.S. Ok), meththika@sjp.ac.lk (M. Vithanage).

https://doi.org/10.1016/j.eti.2020.100847
2352-1864/

(EDCs), collectively known as emerging contaminants (ECs). ECs are excessively released into the environment from household waste, agricultural activities, hospitals, veterinary clinics, wastewater treatment plants, sewage treatment plants, landfills etc. due to regular and immense use of anthropogenic chemicals and PPCPs (Balakrishna et al., 2017). Various monitoring activities have demonstrated the existence of recalcitrant pollutants in various water sources at concentrations ranging from dozens of ng $L^{-1}$ to thousands of $\mu g\ L^{-1}$ (Odendaal et al., 2015). These ECs are, in general, biologically active, water-soluble, and essentially non-biodegradable; therefore, currently, they are frequently detected in environmental waters. Among many different ECs, caffeine (CFN) is one of the most commonly used emerging substance. It is included in the list of PPCPs and used as stimulant drugs (Lee et al., 2019), psychoactive agents (Kumar et al., 2019), and additive in drugs to increase the analgesic effects (Beltrame et al., 2018). It is also used as a personal care product in cosmetic products (Herman and Herman, 2012).

CFN is frequently detected in the environmental water due to its high solubility in aqueous medium (21.6 g $L^{-1}$), high range of half-life up to 100 day, and low octanol-water partition coefficient (Log Kow = 0.16) (Álvarez Torrellas et al., 2016). Many research and review papers have reported that CFN has been frequently found in effluent of embalming process at concentration as high as 14.20 mg $L^{-1}$ (Kleywegt et al., 2019), wastewater at 0.3 $\mu g\ L^{-1}$ (Loos et al., 2013), groundwater at a concentration of 189–505 ng $L^{-1}$ (Kumar et al., 2019; Luo et al., 2014). Further, urinary excretions have reported CFN at high concentrations; 11.4 mg $L^{-1}$ (Rybak et al., 2015) and 14 mg $L^{-1}$ (van der Merwe, 1988). Moreover, the occurrence of CFN in the aquatic environment has been increased year-by-year. For instance, in wastewater, concentration of CFN was 159 ng $L^{-1}$ in 2018 (Ma et al., 2018), while it was found as 6.2 $\mu g\ L^{-1}$ in 2019 (Ashfaq et al., 2019), and in 2020, it is reported as 0.21 mg $L^{-1}$ (Picó et al., 2020). Although many advanced technologies such as photolysis ultraviolet, vacuum ultraviolet, chemically modified vacuum ultraviolet, (Sun et al., 2019) nano-filtration membrane Xu et al. (2019) have employed effectively in the removal of PPCPs from the aquatic environment, they are not economically viable in the removal of PPCPs. This has directed the research on finding effective adsorbents, viable for removing CFN from wastewater. Although there are many eco-friendly adsorbents, such as activated carbon, which have been employed in treating wastewater, however the production of activated carbon is expensive due to its high energy requirements (Zhang et al., 2015). Therefore, attention has been given to biochar as a sorbent for environmental management.

Biochar is derived from the thermal decomposition (pyrolysis) of biological residues, such as plant materials, manure, and household waste, under a limited oxygen environment at a moderate temperature of 200–900 °C (Ahmad et al., 2014; Bastidas-Oyanedel and Schmidt, 2018; Brassard et al., 2019). Biochar is an eco-friendly, low-cost, and carbon-rich material that has been researched extensively for the removal of various contaminants from wastewater including adsorptive removal of pharmaceuticals in human urine (Bordoloi et al., 2017; Solanki and Boyer, 2017). Biochar pyrolyzed at 700 °C has been shown to have more aromatic character than that pyrolyzed at 300 °C. This trait accounts for the decrease in the hydrophilic character of the surface of the biochar, which enables the adsorption of organic contaminants from the aquatic environment (Rajapaksha et al., 2014). The adsorption capacity of biochar has frequently been further improved through chemical and physical activation following pyrolysis (Zhang et al., 2014). Physical activation process is more preferable over chemical activation, since the chemical process needs harmful chemicals in order to improve the surface properties. Moreover, the steam activation process further promotes the formation and distribution of the pores on the surface of biochar than carbon dioxide activation (Zhang et al., 2014). For example, a recent study revealed that steam activation had enhanced the surface area of activated carbon than carbon dioxide (Iruretagoyena et al., 2020). A similar observation was obtained by San Miguel et al. (2003). Steam may activate the biochar by oxidizing its surface, thus removing ash, and thereby, increasing the surface area.

The steam activated biochar exhibited promising adsorption capacity to the organic pollutants from the aquatic environment. For instance, the steam activated biochar, derived from the invasive plant pyrolyzed at 700 °C, showed the highest adsorption capacity (37.73 mg $g^{-1}$) than its pristine biochar (20.56 mg $g^{-1}$) toward the adsorption of sulfamethazine (Rajapaksha et al., 2015). Similarly, Mayakaduwa et al. (2017) reported the highest removal of carbofuran by steam activated rice husk biochar (160.77 mg $g^{-1}$) than the pristine rice husk biochar (132.87 mg $g^{-1}$), produced at 700 °C.

With the exception of water, tea is the second most consumed beverage in the world. In 2010, the annual tea production was reported as 4.52 million tons worldwide and in 2012, 0.3 million tons in Sri Lanka alone (Li and Zhu, 2015). As a result, infused tea residue is a biowaste product; however, it may be converted into a valuable adsorbent. It has been reported that tea waste contains $\approx$ 18.57% fixed carbon, 25.68% lignin, 31.05% holocellulose, and 48.6% carbon (Uzun et al., 2010). This composition may create a more porous structure and provides higher aromatic character to the biochar surface during pyrolysis. Tea-waste biochar has been used to remove organic contaminants, such as carbofuran (Mayakaduwa et al., 2016) and sulfamethazine (Rajapaksha et al., 2014), from aqueous media, exhibiting promising results. Steam-activated tea-waste biochar (TWBC-SA) has also been demonstrated to have a promising adsorption capacity (24.6 mg $g^{-1}$) than its pristine biochar (2.7 mg $g^{-1}$), produced at the same operational condition to remove sulfamethazine from aqueous media (Rajapaksha et al., 2014). However, no literature on the adsorption of CFN onto steam-activated biochar is available to the knowledge of the authors. Therefore, the objectives of this study were to (1) assess the adsorption capacity of engineered TWBC-SA for CFN through batch experiments under different operational parameters such as, solution pH, initial concentration of CFN, and contact time; and (2) analyze the resulting adsorption isotherm and kinetic data to propose a plausible adsorption mechanism for CFN removal from an aqueous environment by TWBC-SA.

## 2. Materials and methods

### 2.1. Chemicals

CFN (98.5%) was purchased from Sisco Research Laboratories Pvt., Ltd. (Mumbai, India). HCl and NaOH, used to adjust the pH of the solutions, and KBr, used to prepare pellets for the Fourier-transform infrared spectroscopy (FTIR) analyses, were purchased from Sigma-Aldrich (St. Louis, MO).

### 2.2. Biochar production and characterization

Waste tea residue was collected, rinsed with deionized water, air-dried, and ground into particles $\leq$0.1 mm in size. It was then pyrolyzed at 700 °C to obtain tea-waste biochar via slow pyrolysis for 2 h by heating at an increased rate of 7 °C $min^{-1}$ under limited $O_2$. After pyrolysis, the biochar was activated under a flow of steam at 5 mL $min^{-1}$ for 45 min at the peak temperature (700 °C) and atmospheric pressure to produce TWBC-SA. Generally, the steam can generate new porous structure by eliminating the ash and incomplete combustion of particles (Rajapaksha et al., 2015), and also it can oxidize the surface of biochar by releasing hydrogen, carbon monoxide, and carbon dioxide, resulting enhancement of surface properties (Manyà, 2012). The KBr-pellet transmittance spectra of the pristine TWBC-SA and CFN-adsorbed TWBC-SA were obtained to investigate the influence of functional groups before and after CFN adsorption using a Nicolet iS10 FTIR spectrometer (Thermo Fisher Scientific, Waltham, MA). Data were collected in the range of 4000–500 $cm^{-1}$, with 64 repetitive scans and a resolution of 4 $cm^{-1}$. Baseline correction, peak assignment, and noise reduction were assessed using OMNIC software 6.0 (Thermo Fisher Scientific, Waltham, MA). The morphology of the surface of the biochar was investigated using an analytical variable pressure field emission scanning electron microscope (SU6600 FESEM; Hitachi, Ltd., Tokyo, Japan). Samples were prepared by placing a minute amount of the biochar on a sample stub and sputter-coating with gold. The composition of the chemical elements on the surface of the TWBC-SA before and after CFN adsorption was further studied using X-ray photoelectron spectroscopy (XPS) (ESCALAB Xi; Thermo Fisher Scientific, Waltham, MA) with an Al monochromatic X-ray radiation source at 12 mA and 14 kV.

### 2.3. pH-adsorption edge experiments

Adsorption studies were conducted using 100 mL of CFN solution (although, CFN has been detected in the environment at lower concentration range, ranging from μg $L^{-1}$ (Phan et al., 2015) to mg $L^{-1}$ (Li et al., 2020), a higher (50 mg $L^{-1}$) initial concentration of CFN was used in this study, to assess the viability and maximum affinity of engineered TWBC-SA toward the CFN in the aqueous media) and 100 mg of TWBC-SA under a nitrogen-purged environment, which reduced the interference of atmospheric carbon dioxide on the pH of the media, at room temperature (25 °C). A mixture of 50 mg $L^{-1}$ CFN and TWBC-SA was kept in a plate shaker for 12 h to attain the equilibrium. The influence of pH on the adsorption of CFN onto TWBC-SA was studied in the pH range of 3–10. The pH of the solutions was adjusted using 0.1 M HCl and 0.1 M NaOH solutions. Finally, the mixtures were centrifuged at 500 rpm and filtered through 0.45 μm syringe filters (Labfil PTFE hydrophobic, C0000300; ALWSCI, China). Residual concentrations of CFN in the solutions were determined spectrophotometrically using a GENESYS 10S UV–Vis spectrophotometer (Thermo Fisher Scientific, Waltham, MA) at a $\lambda_{max} = 272$ nm.

### 2.4. Adsorption kinetic experiments

Kinetic adsorption studies were performed using 50 mg $L^{-1}$ initial concentration CFN solutions with 1 g $L^{-1}$ doses of TWBC-SA. The pH of the solutions and temperature was maintained at 3.5 (optimum pH) and 25 °C, respectively. During the experiments, the contact time of TWBC-SA with CFN solution was varied between 5 min and 24 h. Finally, each solution was centrifuged, filtered, and analyzed for the equilibrium concentration of CFN.

### 2.5. Adsorption isotherm experiments

Isotherm experiments were conducted using different initial concentrations of CFN (10, 15, 25, 50, 100, 150, 225, and 300 mg $L^{-1}$), with an adsorbent (TWBC-SA) dose of 1 g $L^{-1}$, at pH 3.57 (optimum pH obtained from the pH-adsorption edge experiments), at room temperature (25 °C), with a contact time of 12 h. Solutions were centrifuged and filtered before analysis. Batch experiments were carried out in triplicate, and the results were averaged.

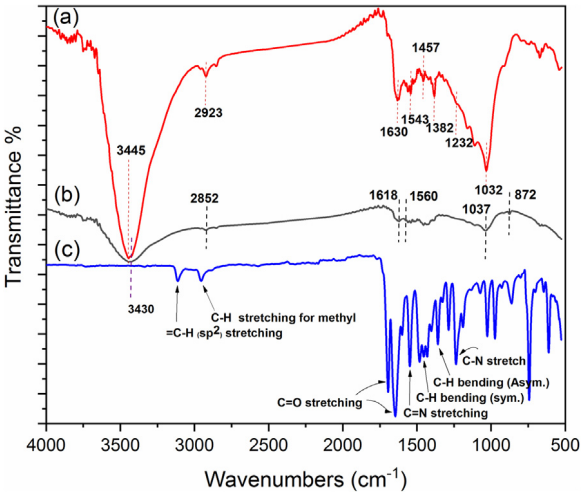


**Fig. 1.** FTIR spectra (KBr) of: (a) TWBC-SA after CFN adsorption, (b) pristine TWBC-SA (before CFN adsorption), and (c) CFN.

### 2.6. Data modeling

Kinetic modeling was conducted using non-linear pseudo-second-order and Elovich equations. Isotherm modeling was performed using non-linear form of Temkin and Freundlich isotherm equations to understand the adsorption mechanism of CFN by TWBC-SA. Experimental data modeling was conducted using Origin 8.0 statistical computer software.

The amount of CFN adsorbed by TWBC-SA ($q_e$; mg $g^{-1}$) and the adsorbed percentage of CFN ($A\%$) can be calculated using Eqs. (1) and (2), respectively (Li et al., 2018; Vithanage et al., 2016).

$$q_e = \frac{(C_o - C_e)}{m} v \tag{1}$$

$$A\% = \frac{(C_o - C_e)}{C_o} 100\% \tag{2}$$

where, $C_o$ is the initial concentration of CFN in mg $L^{-1}$, $C_e$ is the equilibrium concentration of CFN in mg $L^{-1}$, $v$ is the volume of solution in L, and $m$ is the amount of adsorbent (TWBC-SA) in g.

## 3. Results and discussion

### 3.1. Biochar characterization

Transmittance FTIR spectra of CFN saturated TWBC-SA (after CFN adsorption), pristine TWBC-SA (before CFN adsorption), and CFN are illustrated in Fig. 1((a), (b), and (c), respectively). The FTIR spectrum of the pristine TWBC-SA (Fig. 1(b)) revealed that the broad vibrational peak at 3430 $cm^{-1}$ belonged to the hydroxyl stretching vibration of a phenolic group (Chen et al., 2008). This might be due to the presence of lignin and holocellulose in the biochar (Uzun et al., 2010). The characteristic peaks obtained at 2852, 1618, 1560, 1037, and 872 $cm^{-1}$ were attributed to the C–H stretching frequencies of a methyl group attached to an aromatic ring (Uzun et al., 2010), C=O stretching, aromatic C=C stretching, alcoholic C–O and C–O–C stretching, and out-of-plane aromatic C–H bending vibrations, respectively (Uzun et al., 2010). This was further confirmed by the XPS spectra shown in Fig. 2. Peaks for C 1s, N 1s, and O 1s were observed at 284.88, 399.72, and 532.1 eV, respectively, indicating the presence of C, N, and O on the TWBC-SA (Liu et al., 2020). Furthermore, the observed characteristic peaks at 348.26, and 1304.6 eV corresponding to Ca, and Mg respectively (Liu et al., 2020).

The surface properties of the biochar were found to improve through steam activation. The general reaction that took place on the surface of the tea-waste biochar during the steam activation process is shown in Figure 1S (supplementary file).

SEM images were photographed at various resolutions to investigate the porous characteristics and surface morphology features of TWBC-SA (Fig. 3). It can be seen that the TWBC-SA has a very well-developed, porous surface (pore volume and diameter = 0.1091 $cm^3$ $g^{-1}$ and 1.998 nm, respectively). This porous structure on the surface of the biochar may lead to its high surface area (576 $m^2$ $g^{-1}$) (Rajapaksha et al., 2014). The distribution of the pores on the surface of TWBC-SA play an important role in the adsorption of CFN onto the TWBC-SA. The higher the surface area of the biochar, the more will be the adsorption (Hassan et al., 2020).

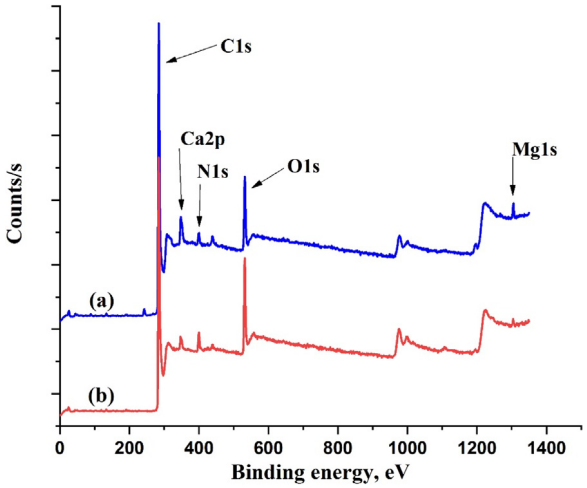


**Fig. 2.** X-ray photoelectron spectra of: (a) TWBC-SA before CFN adsorption and (b) TWBC-SA after CFN adsorption.

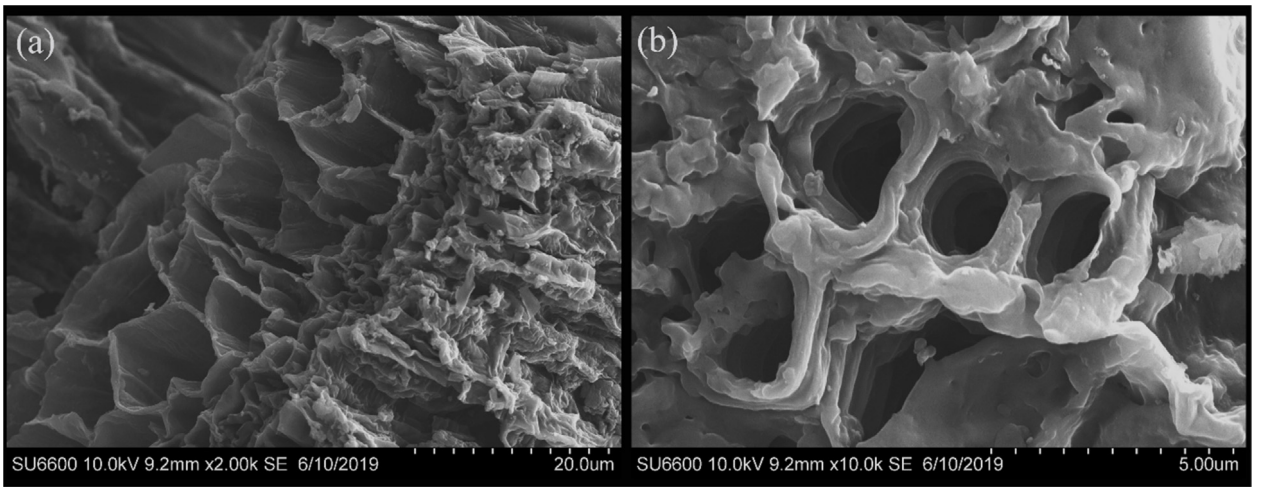


**Fig. 3.** SEM images of the TWBC-SA at: (a) 2.00k× and (b) 10.00k× magnifications.

### *3.2. Effect of solution pH on the CFN adsorption*

The pH of the solution is an important parameter during the adsorption process. The charge on the surface of the adsorbate and the chemical properties of the adsorbent are dependent on the pH of the solution. It has been reported that CFN exists in the neutral form (CFN) in acidic medium up to pH 5.5. Above pH 5.5, CFN exists in the anionic form ($CFN^-$) (Beltrame et al., 2018). Fig. 4 shows the variation of the adsorption capacity of TWBC-SA for CFN with pH and the speciation of CFN as a function of pH. It was revealed that the highest CFN adsorption occurred at low pH values, between 3.5 and 5.5. At pH values >5.5, adsorption of CFN decreased to a constant level. In the pH range of 3.5–5.5, the neutral form CFN species fraction was close to one. Therefore, in this pH range, adsorption of CFN was the highest because the production of $CFN^-$ was near zero. The maximum adsorption capacity, 15.4 mg $g^{-1}$, was achieved at pH 3.5. At low pH values, the negatively charged surface of the biochar is protonated. The protonated TWBC-SA and neutral form CFN may interact with each other. These interactions are due to non-electrostatic forces, such as hydrogen bonding, under these conditions (Couto et al., 2015). At higher pH values (6–10), $CFN^-$ may interact with the positively charged surface of TWBC-SA (Singh et al., 2017). Under these conditions, the non-electrostatic interactions become less favorable, causing a decrease in the adsorption of CFN.

### *3.3. Effect of contact time on CFN adsorption*

The kinetic studies are important to establish the equilibration time for the maximum uptake of pollutant and to know the kinetics of the adsorption process. The adsorption capacity of TWBC-SA for CFN increased rapidly until 90 min, then

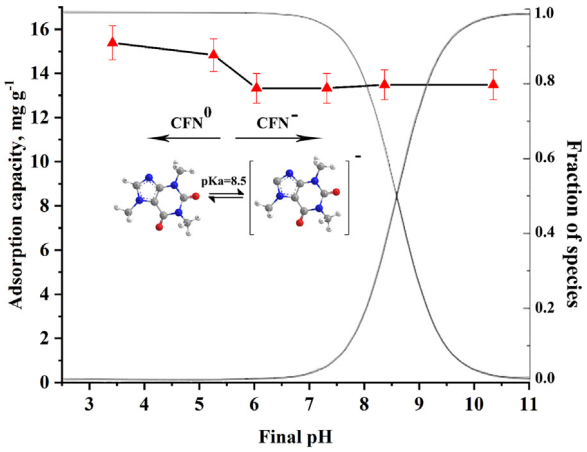


**Fig. 4.** Variation of the adsorption capacity of TWBC-SA for CFN with final pH of the solution (25 °C, TWBC-SA dose = 1 g $L^{-1}$, and $C_o$ = 50 mg $L^{-1}$), along with speciation diagrams of CFN as a function of pH. (The error bars represent the estimated ± standard error of mean (n = 3)).

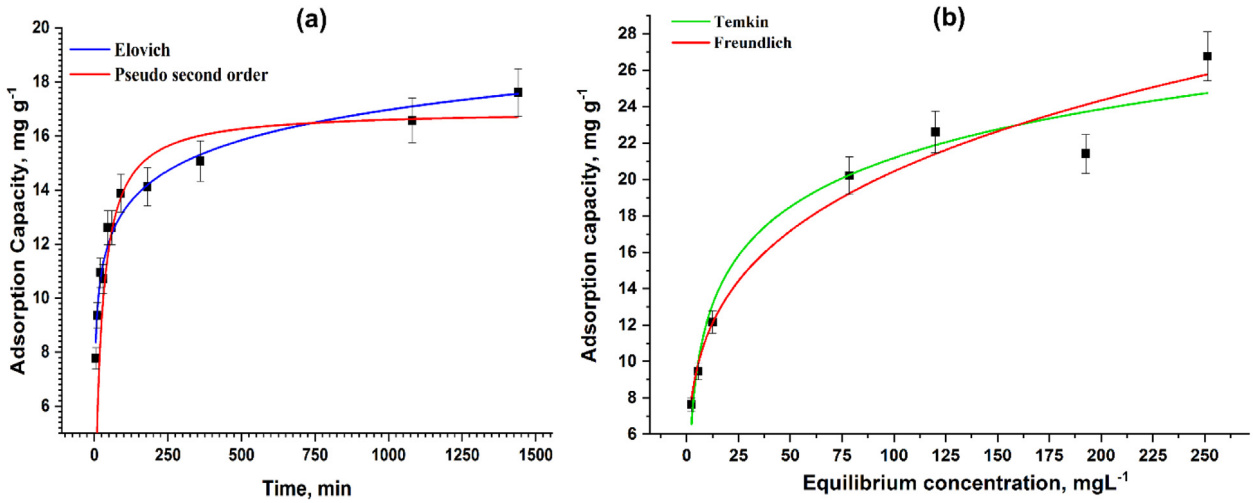


**Fig. 5.** Model fitting of the adsorption batch experiments: (a) kinetic modeling of the adsorption of CFN onto TWBC-SA at pH 3.5 (initial concentration of CFN = 50 mg $L^{-1}$ and TWBC-SA dose = 1 g $L^{-1}$); and (b) isotherm modeling of the adsorption of CFN onto the TWBC-SA at pH 3.5 (contact time = 12 h and TWBC-SA dose = 1 g $L^{-1}$ at 25 °C). (The error bars represent the estimated ± standard error of mean (n = 3)).

reached to equilibrium (Fig. 5(a)). The Elovich and pseudo-second-order kinetic model fittings of the data (Fig. 5(a)) and the values of the parameters used (Table 1) clearly indicate that the Elovich model fitted well to the experimental data ($R^2$ = 0.972). The data fitting of Elovich equation suggests that the adsorption of CFN onto the heterogeneous surface of TWBC-SA is driven by chemisorption (Ashiq et al., 2019). According to the results from the Elovich model, the initial rate constant of adsorption ($\alpha$) was 55.66 mg $g^{-1}$ $min^{-1}$. This indicative the adsorption of CFN by TWBC-SA was a random process since the vacant active sites on TWBC-SA were higher at the beginning. Afterwards, the adsorption reaches to equilibrium as a result of the filling of adsorption sites on the surface of the TWBC-SA and only limited sites are left for further adsorption (Seneviratne et al., 2015), producing a desorption constant ($\beta$) = 0.62 g $mg^{-1}$. Thus, the high $\alpha$ and low $\beta$ values specify the favorability of adsorption of CFN onto the surface of TWBC-SA (Chien and Clayton, 1980).

### *3.4. Effects of initial CFN concentration*

The adsorption isotherm can be described as the relationship between the amount of CFN adsorbed onto TWBC-SA and the residual concentration of CFN, remained in the aqueous phase. The adsorption capacity of TWBC-SA for CFN was found to increase (7.64 to 26.77 mg $g^{-1}$) with increasing initial CFN concentration (Fig. 5(b)). However, the adsorption percentage of CFN decreased (77.07 to 9.62%) with increasing initial CFN concentration. The adsorption isotherm models were fitted to the experimental data and results are presented in Fig. 5(b). The results show that the number of CFN molecules at low initial concentrations is lower than the available active sites on the surface of the TWBC-SA. Therefore,

**Table 1**
Kinetic and isotherm model parameters for the adsorption of CFN onto the TWBC-SA at pH 3.5.

| Kinetic model fittings | | |
|---|---|---|
| Models | Parameters | Values |
| Elovich | $\alpha$ (mg $g^{-1}$ $min^{-1}$) | 55.590 |
| | $\beta$ (g $mg^{-1}$) | 0.615 |
| | $R^2$ | 0.972 |
| | $Chi^2$ | 0.258 |
| Pseudo-second order | $k_2$ (g $mg^{-1}$ $min^{-1}$) | 0.003 |
| | $q_{e\,(calculate)}$ (mg $g^{-1}$) | 16.957 |
| | $q_{e\,(experiment)}$ (mg $g^{-1}$) | 17.611 |
| | $R^2$ | 0.784 |
| | $Chi^2$ | 0.537 |
| Isotherm model fitting | | |
| Temkin | b | 640.976 |
| | $A_T$ (L $mg^{-1}$) | 2.399 |
| | $R^2$ | 0.955 |
| | $Chi^2$ | 2.457 |
| Freundlich | $K_F$ (mg $g^{-1}$)/(mg $L^{-1}$) $^n$ | 6.430 |
| | n | 0.251 |
| | $R^2$ | 0.960 |
| | $Chi^2$ | 2.183 |

the adsorption of CFN by TWBC-SA is dependent on the initial concentration of CFN in the solution (Seneviratne et al., 2015). The L-curve in Fig. 5(b) shows the affinity of CFN for TWBC-SA. In the beginning of the process, the adsorption process was rapid as more adsorption sites on TWBC-SA surface were available for CFN adsorption. Later, as more active sites on the TWBC-SA surface were filled, it became increasingly difficult for the CFN molecules to find the vacant sites and process became slow (Lawrence et al., 2000).

The experimental data were fitted to the non-linear models of Temkin and Freundlich. All of the isotherm parameters, coefficients of determination ($R^2$), and $Chi^2$ values of each model are summarized in Table 1. Based on $R^2$ and $Chi^2$ values, the best-fitting isotherm model for the experimental data can be suggested, having a high $R^2$ and low $Chi^2$ value (Mayakaduwa et al., 2016). Values of $R^2 > 0.95$ and $Chi^2 < 2.5$ were used. Based on these parameters, the best-fitting model was the Freundlich model (Table 1). The Freundlich model describes physisorption interactions occurring at the surface of the adsorbent, heterogeneously, having different affinities. Generally, the Freundlich model depicts the favorability of the adsorption of CFN in terms of adsorption intensity (n). When $n = 1$, the adsorption is independent of CFN concentration, while $0 < n < 1$ indicates favorable adsorption, and $n > 1$ indicates unfavorable adsorption (Seneviratne et al., 2015). The adsorption of CFN by TWBC-SA is favorable in this study, since $n = 0.251$.

The non-linear Temkin isotherm model, shown in Fig. 5(b), describes the interaction of the adsorbate with the adsorbent as being due to a chemisorption process, expressing it in terms of the heat of adsorption (B; 3.865 J $mol^{-1}$), calculated using Eq. S3 (supplementary file). This value indicates that the energy of adsorption is linearly associated with coverage due to the interactions between CFN and TWBC-SA (Biswas et al., 2007; Rajapaksha et al., 2015). The $R^2$ and $Chi^2$ values of this model were 0.955 and 2.457, respectively, suggesting that the adsorption of CFN onto the TWBC-SA surface was driven by mixed mechanisms involving chemical and physical forces (Biswas et al., 2007). The values of the parameters use for this model are summarized in Table 1.

### 3.5. Comparison of CFN adsorption by various adsorbents

The adsorption of CFN by various adsorbents, such as activated carbon (Sotelo et al., 2014), activated carbon fiber (Beltrame et al., 2018), and carbon xerogel (Ptaszkowska-Koniarz et al., 2018) has been well studied previously. The adsorption capacity of TWBC-SA for CFN was compared to these adsorbents (Table 2). Activated carbon showed a higher CFN adsorption capacity than that of TWBC-SA as activated carbon has a very high surface area. Even though the surface areas of TWBC-SA and carbon xerogel are similar, the adsorption capacity of TWBC-SA for CFN was lower than that of the carbon xerogel. However, the production of activated carbon, activated carbon fiber, and carbon xerogel requires many chemicals and is very expensive due to the high energy requirements during production. Therefore, the utilization of environmental waste in the production of potential adsorbents for the remediation of contaminants in a low-cost manner is highly appreciated. The fique bagasse biochar, produced at different pyrolysis temperatures (650, 750, and 850 °C), exhibited the adsorption capacity of CFN as 3.52–9.13 mg $g^{-1}$ (Correa-Navarro et al., 2019). Similarly, woodchip biochar showed an adsorption capacity of 13.2 mg $L^{-1}$ for CFN removal from wastewater (Muter et al., 2019). However, TWBC-SA from tea residue was successfully engineered in a low-cost manner and has been shown to effectively remove CFN from an aqueous environment in this study than the available information in the literature.

**Table 2**
Comparison of CFN adsorption by the TWBC-SA and various previously studied adsorbents.

| Adsorbents | $C_o$ of CFN (mg $L^{-1}$) | Dosage of adsorbent (g $L^{-1}$) | Surface area ($m^2$ $g^{-1}$) | Optimum pH | Adsorption capacity (mg $g^{-1}$) | References |
|---|---|---|---|---|---|---|
| Carbon xerogel modified with copper acetate | 6.5–150 | 0.4 | 546 | ~2.0 | 107.0 | Ptaszkowska-Koniarz et al. (2018) |
| Carbon xerogel | 100 | – | 367 | – | 79.1 | Álvarez et al. (2015) |
| Mesoporous activated carbon fibers | 500 | 1 | 1031 | ~6.0 | 155.5 | Beltrame et al. (2018) |
| Chemical-activated carbons | 100 | 0.12 g | 1216 | – | 40.0 | Torrellas et al. (2015) |
| Granular activated carbon | 50 | – | 997.0 | – | 190.9 | Sotelo et al. (2014) |
| Fique bagasse biochar | 100 | 10 | – | 2.0 | 9.12 | Correa-Navarro et al. (2019) |
| TWBC-SA | 50 | 1 | 576.09 | 3.5 | 15.4 | **This study** |

### 3.6. Adsorption mechanism

Several adsorption mechanisms, including $\pi$-$\pi$, dipole–dipole, hydrogen bonding, and electrostatic attraction interactions, have been suggested in the removal of inorganic and organic contaminants from the aquatic environment (Ahmad et al., 2014; Tran et al., 2017). The results of this study suggest that the adsorption of CFN onto TWBC-SA occurs mainly due to a chemisorption process. This is further evidenced by the FTIR and XPS analyses before and after the adsorption of CFN onto TWBC-SA. As shown in Figs. 1, and 2, notable changes were observed in the peaks of CFN saturated TWBC-SA (after CFN adsorption), which were not present in those of the pristine TWBC-SA (before CFN adsorption).

In FTIR spectra (Fig. 1), the appearance of C–H characteristic stretching band of a methyl group at 2923 $cm^{-1}$, C–H bending (symmetry) at 1457 $cm^{-1}$, and C–H bending (asymmetry) at 1382 $cm^{-1}$ (Donald et al., 2001) for CFN-adsorbed TWBC-SA sample indicates the presence of CFN molecules on the adsorbent surface. Further, the presence of C=O characteristic stretching band for CFN at 1630 $cm^{-1}$(Vithanage et al., 2016) for CFN-adsorbed TWBC-SA sample indicates the existence of CFN on TWBC-SA surface. Additionally, C=N stretching peak at 1543 $cm^{-1}$ and C–N stretching band at 1232 $cm^{-1}$ (Chen et al., 2012) for CFN-adsorbed TWBC-SA sample further confirmed the presence of CFN on the adsorbent surface. In contrast, these peaks are not present for the pristine TWBC-SA, confirming the successful incorporation of CFN molecules onto the surface of the TWBC-SA (Fig. 1).

Moreover, Fig. 6 shows the narrow-scan deconvolution XPS spectra of C 1s, N 1s, and O 1s before and after the adsorption of CFN onto TWBC-SA. Fig. 6(a) and (b) show the C 1s peaks for pristine and CFN-loaded TWBC-SA, respectively. The peak appearing at 284.8 eV represents C of C–C and C–H functional groups (Pang et al., 2010). The peak corresponding to C of C–N (N-$sp^3$ C hybridization) appears at a binding energy = 286.25 eV (Liu et al., 2020). The binding energy peaks observed at 287.35 eV are ascribed to the C of –COOC, C=O, and N–C=O functional groups (Li et al., 2018). The N 1s peaks of pristine and CFN-loaded TWBC-SA are shown in Fig. 6(c) and (d), respectively. The peaks are seen at 398.8 and 400.8 eV represents N of C–N (Li et al., 2018) and N–C=O (Afzal et al., 2019) groups, respectively. Fig. 6(e) and (f) represent the O 1s peaks of pristine and CFN-loaded TWBC-SA, respectively. The peaks at 531.7 and 533.75 eV are attributed to the O of C=O and C–O (Li et al., 2018), respectively.

No new peaks were observed in the XPS spectra of TWBC-SA after the adsorption of CFN. However, an increase in the intensities of existing peaks, a blueshift of the peaks in the N 1s, and redshift of the peaks in the C 1s, and O 1s regions (Table 3) were observed after the adsorption of CFN by TWBC-SA. These observations might demonstrate that CFN successfully loaded onto the TWBC-SA. The atomic percentage of the peak corresponding to the C of a C–N (N-sp3 C hybridization) group at 286.25 eV increased by 2.03% (Table 3). This change in the atomic percentage after CFN adsorption was most likely due to the interactions of CFN molecules with the surface of the TWBC-SA. Likewise, the increase in the intensity of the C peak of N–C=O at 287.35 eV by 0.27% also indicates the interaction of CFN with TWBC-SA surface. Furthermore, the N peak intensities corresponding to N–C and N–C=O groups at 398.8 and 400.8 eV, respectively, increased by 0.38 and 1.64%, showing the successful interaction of CFN with TWBC-SA (Table 3). Additionally, the O peak intensity corresponding to a C=O group at 531.7 eV sufficiently increased by 2.55%, further elaborating the successful incorporation of CFN onto TWBC-SA surface.

CFN might have undergone structural changes during the adsorption process wherein one of the C=O stretching characteristic bands of CFN at 1693 $cm^{-1}$ disappeared in the spectrum of loaded TWBC-SA. Furthermore, the high-intensity peaks of hydroxyl group at 3445 $cm^{-1}$, and C–O and C–O–C stretching bands at 1032 $cm^{-1}$ (Emeka et al., 2014) may confirm the formation of new –OH, and C–O and/or C–O–C groups on the CFN adsorbed TWBC-SA. Besides, the formation of a C–O bond after CFN adsorption can also be seen in the XPS data. The C peak belongs to C–O at 286.25 eV and O peak corresponding to C–O at 533.75 eV increased by 2.03, and 3.45% respectively (Table 3), indicating that CFN underwent

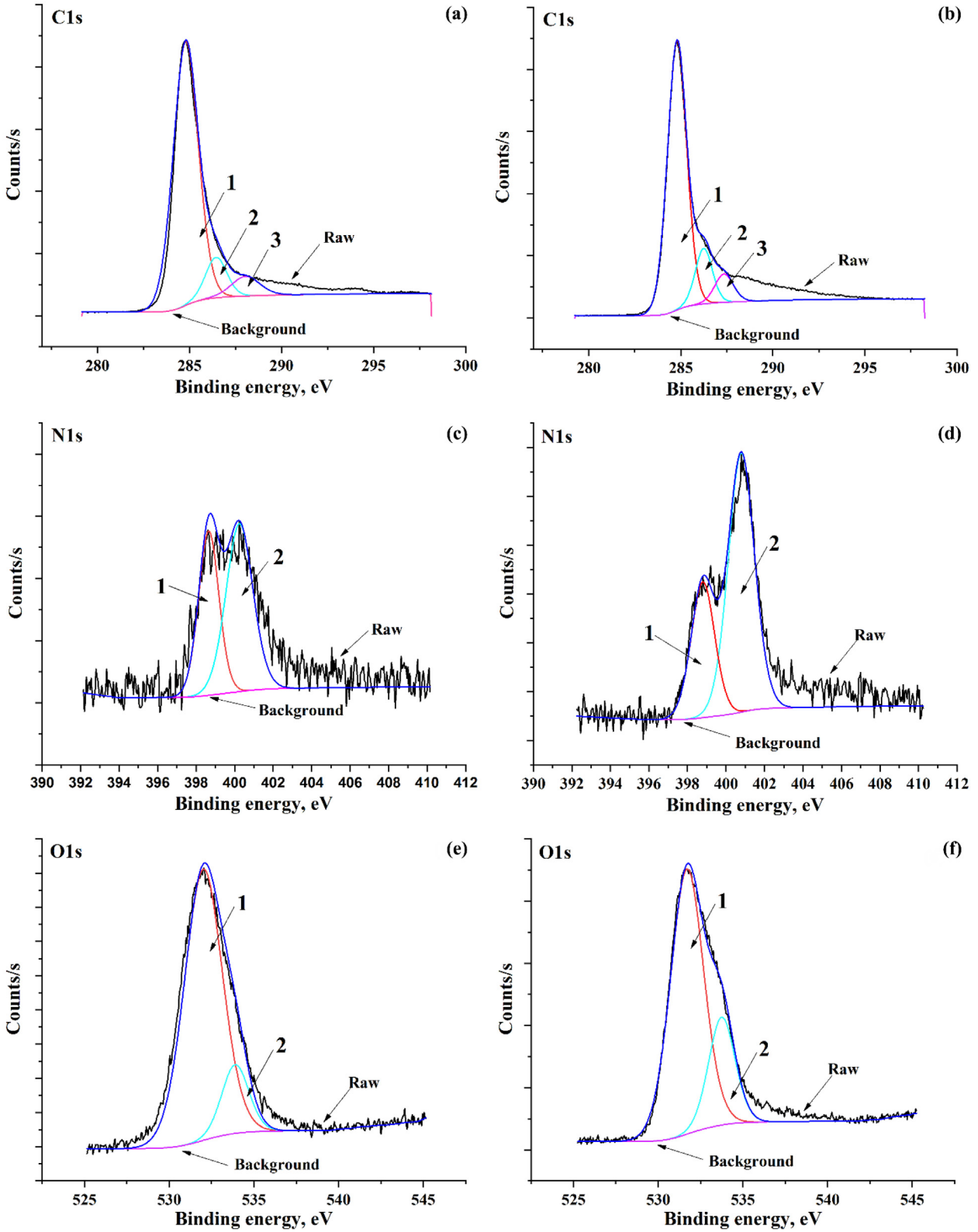


**Fig. 6.** Narrow-scan XPS spectra of the pristine TWBC-SA (left) and CFN-adsorbed TWBC-SA (right): (a) and (b) C 1s, (c) and (d) N 1s, and (e) and (f) O 1s, * functional groups belong to peaks 1, 2, and 3 are represented in Table 3.

**Table 3**
The atomic percentage of C, N, and O containing functional groups on the TWBC-SA before and after CFN adsorption[a].

| Elements | Peaks | TWBC-SA | | CFN-adsorbed TWBC-SA | | Functional groups |
|---|---|---|---|---|---|---|
| | | Peak position (eV) | Atomic % | Peak position (eV) | Atomic % | |
| C 1s | 1 | 284.80 | 72.00 | 284.80 | 63.11 | C–C, C–H |
| | 2 | 286.45 | 09.49 | 286.25 | 11.52 | C–N (N-sp$^3$C), C–O |
| | 3 | 288.05 | 06.18 | 287.35 | 06.45 | –COOC, C=O, N–C=O |
| N 1s | 1 | 398.65 | 01.08 | 398.80 | 01.46 | N–C |
| | 2 | 400.25 | 01.47 | 400.80 | 03.11 | N–C=O |
| O 1s | 1 | 532.02 | 08.30 | 531.70 | 10.85 | C=O, O=C–O |
| | 2 | 533.90 | 0.07 | 533.75 | 03.52 | C–O |

[a]All of the peaks are shown in Fig. 6.

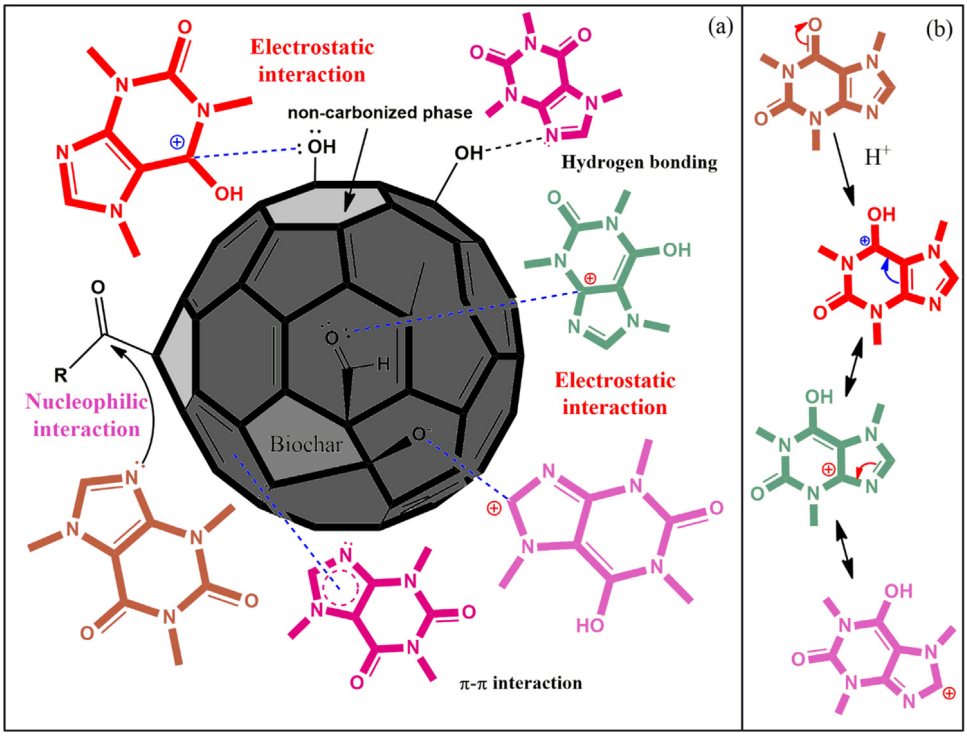


**Fig. 7.** (a) A plausible mechanism for CFN adsorption onto TWBC-SA and (b) resonance of the ionized CFN molecule.

chemical changes during the adsorption process. As shown in Fig. 7, one of the C=O groups of the CFN molecule was converted to a hydroxyl group during adsorption of CFN by TWBC-SA. This observation is corroborated by the FTIR spectra (Fig. 1(a) and (b)). This observation revealed that CFN was successfully adsorbed by TWBC-SA through the chemisorption process.

The experiment data of present study, suggest that the adsorption of CFN onto TWBC-SA was driven by aromatic hydroxyl and carbonyl groups, present on the biochar surface. The carbonyl groups on TWBC-SA surface have the capability of undergoing nucleophilic attack (Mayakaduwa et al., 2016). In an acidic medium, the nitrogen atom of the five-membered ring of CFN molecule (Fig. 7) might undergo a nucleophilic addition reaction with the carbonyl groups present on TWBC-SA surface. The plausible reaction mechanism that is expected to take place is illustrated in Fig. 7. At the same time, there might be physisorption of CFN occurring on TWBC-SA surface, which is driven by $\pi$-$\pi$ and hydrogen bonding interactions between the surface of TWBC-SA and the heterocyclic ring of the CFN molecule.

## 4. Conclusions

In this study, engineered tea-waste biochar-steam activated (TWBC-SA) was successfully applied for the adsorption of CFN from aqueous media. The TWBC-SA surface was found to possess a high aromatic character. Multi-resolution SEM images of TWBC-SA confirmed the formation and distribution of porous structures on the surface of TWBC-SA during pyrolysis. The highest adsorption of CFN occurred at pH 3.5. The adsorption capacity was slightly decreased until pH 5.5.

Above pH 5.5, the adsorption of CFN was pH-independent. It is assumed that at lower pH values, there may be non-electrostatic interactions between the neutral form of CFN molecule and the protonated surface of TWBC-SA. Isotherm and kinetic results indicated that chemisorption mainly governed the removal of CFN by TWBC-SA. Chemisorption was triggered via nucleophilic addition, the formation of covalent bonds, and electrostatic attraction, which were confirmed by FTIR and XPS analyses. However, physisorption was a supportive mechanism to that of chemisorption in the removal of CFN from the aqueous environment, involving $\pi$-$\pi$ and hydrogen bonding interactions between the surface of TWBC-SA and the heterocyclic ring of the CFN molecule. Overall, this study suggests that the engineered steam-activated tea-waste biochar can be used as a potential adsorbent for CFN removal from aqueous media. Future studies should investigate CFN adsorption by biochar under relevant environmental conditions such as the realistic concentration of CFN, found in the environment, environmental pH, and CFN removal from the real wastewater. Thus, biochar can be an effective material for treatment of wastewater with urine in municipal treatment plants.

## CRediT authorship contribution statement

**S. Keerthanan:** Writing - original draft, Formal analysis, Writing - review & editing. **Amit Bhatnagar:** Writing - review & editing. **Kushani Mahatantila:** Resources, Writing - review & editing, Supervision. **Chamila Jayasinghe:** Project administration, Writing - review & editing, Supervision. **Yong Sik Ok:** Writing - review & editing. **Meththika Vithanage:** Conceptualization, Supervision, Funding acquisition, Writing - review & editing.

## Declaration of competing interest

The authors declare that they have no known competing financial interests or personal relationships that could have appeared to influence the work reported in this paper.

## Acknowledgments

Authors acknowledge research funding (ASP/01/RE/SCI/2018-65) provided by the Research Council, and analytical facilities of Instrument Center, Faculty of Applied Sciences, University of Sri Jayewardenepura.

## Appendix A. Supplementary data

Supplementary material related to this article can be found online at https://doi.org/10.1016/j.eti.2020.100847.

## References

Afzal, M.Z., Yue, R., Sun, X.F., Song, C., Wang, S.G., 2019. Enhanced removal of ciprofloxacin using humic acid modified hydrogel beads. In: Journal of Colloid and Interface Science. Elsevier Inc., http://dx.doi.org/10.1016/j.jcis.2019.01.083.

Ahmad, M., Rajapaksha, A.U., Lim, J.E., Zhang, M., Bolan, N., Mohan, D., Vithanage, M., Lee, S.S., Ok, Y.S., 2014. Biochar as a sorbent for contaminant management in soil and water: A review. Chemosphere 99, 19–33. http://dx.doi.org/10.1016/j.chemosphere.2013.10.071.

Álvarez, S., Ribeiro, R.S., Gomes, H.T., Sotelo, J.L., García, J., 2015. Synthesis of carbon xerogels and their application in adsorption studies of caffeine and diclofenac as emerging contaminants. Chem. Eng. Res. Des. 95, 229–238. http://dx.doi.org/10.1016/j.cherd.2014.11.001.

Ashfaq, M., Li, Y., Rehman, M.S.U., Zubair, M., Mustafa, G., Nazar, M.F., Yu, C.P., Sun, Q., 2019. Occurrence, spatial variation and risk assessment of pharmaceuticals and personal care products in urban wastewater, canal surface water, and their sediments: A case study of lahore, Pakistan. Sci. Total Environ. 688, 653–663. http://dx.doi.org/10.1016/j.scitotenv.2019.06.285.

Ashiq, A., Adassooriya, N.M., Sarkar, B., Rajapaksha, A.U., Ok, Y.S., Vithanage, M., 2019. Municipal solid waste biochar-bentonite composite for the removal of antibiotic ciprofloxacin from aqueous media. J. Environ. Manag. 236, 428–435. http://dx.doi.org/10.1016/j.jenvman.2019.02.006.

Balakrishna, K., Rath, A., Praveenkumarreddy, Y., Guruge, K.S., Subedi, B., 2017. A review of the occurrence of pharmaceuticals and personal care products in Indian water bodies. Ecotoxicol. Environ. Saf. 137, 113–120. http://dx.doi.org/10.1016/j.ecoenv.2016.11.014.

Bastidas-Oyanedel, J.R., Schmidt, J.E., 2018. Waste biorefinery in arid/semiarid regions. In: Bhaskar, T., Pandey, A., Mohan, S.V., Lee, D.-J., Khanal, S.K. (Eds.), Waste Biorefinery: Potential and Perspectives. Elsevier B.V., pp. 605–621. http://dx.doi.org/10.1016/B978-0-444-63992-9.00020-3.

Beltrame, K.K., Cazetta, A.L., de Souza, P.S.C., Spessato, L., Silva, T.L., Almeida, V.C., 2018. Adsorption of caffeine on mesoporous activated carbon fibers prepared from pineapple plant leaves. Ecotoxicol. Environ. Saf. 147, 64–71. http://dx.doi.org/10.1016/j.ecoenv.2017.08.034.

Biswas, K., Saha, S.K., Ghosh, U.C., 2007. Adsorption of fluoride from aqueous solution by a synthetic iron(III)-aluminum(III) mixed oxide. Ind. Eng. Chem. Res. 46, 5346–5356. http://dx.doi.org/10.1021/ie061401b.

Bordoloi, N., Goswami, R., Kumar, M., Kataki, R., 2017. Biosorption of Co (II) from aqueous solution using algal biochar: Kinetics and isotherm studies. Bioresour. Technol. 244, 1465–1469. http://dx.doi.org/10.1016/j.biortech.2017.05.139.

Brassard, P., Godbout, S., Lévesque, V., Palacios, J.H., Raghavan, V., Ahmed, A., Hogue, R., Jeanne, T., Verma, M., 2019. Biochar for soil amendment. In: Char and Carbon Materials Derived from Biomass: Production, Characterization and Applications. pp. 109–146. http://dx.doi.org/10.1016/B978-0-12-814893-8.00004-3.

Chen, J.Q., Hu, Z.J., Ji, R., 2012. Removal of carbofuran from aqueous solution by orange peel. Desalin. Water Treat. 49, 106–114. http://dx.doi.org/10.1080/19443994.2012.708205.

Chen, B., Zhou, D., Zhu, L., 2008. Transitional adsorption and partition of nonpolar and polar aromatic contaminants by biochars of pine needles with different pyrolytic temperatures. Environ. Sci. Technol. 42, 5137–5143. http://dx.doi.org/10.1021/es8002684.

Chien, S.H., Clayton, W.R., 1980. Application of elovich equation to the kinetics of phosphate release and sorption in soils1. Soil Sci. Soc. Am. J. 44, 265. http://dx.doi.org/10.2136/sssaj1980.03615995004400020013x.

Correa-Navarro, Y.M., Moreno-Pirajáan, J.C., Giraldo, L., Rodríguez-Estupiñan, P., 2019. Caffeine adsorption by fique bagasse biochar produced at various pyrolysis temperatures. Orient. J. Chem. 35, 538–546. http://dx.doi.org/10.13005/ojc/350205.

Couto, O.M., Matos, I., da Fonseca, I.M., Arroyo, P.A., da Silva, E.A., de Barros, M.A.S.D., 2015. Effect of solution pH and influence of water hardness on caffeine adsorption onto activated carbons. Can. J. Chem. Eng. 93, 68–77. http://dx.doi.org/10.1002/cjce.22104.

Donald, L., Pavia, Gary M., Lampman, G.S.K., 2001. Pavia - Introduction to Spectroscopy - Guide for Students of Organic Chemistry 3e (Thomson, 2001).pdf, third ed. Thomson Learning, Inc., USA.

Emeka, E.E., Ojiefoh, O.C., Aleruchi, C., Hassan, L.A., Christiana, O.M., Rebecca, M., Dare, E.O., Temitope, A.E., 2014. Evaluation of antibacterial activities of silver nanoparticles green-synthesized using pineapple leaf (Ananas comosus). Micron 57, 1–5. http://dx.doi.org/10.1016/j.micron.2013.09.003.

Hassan, M., Naidu, R., Du, J., Liu, Y., Qi, F., 2020. Critical review of magnetic biosorbents: Their preparation, application, and regeneration for wastewater treatment. In: Science of the Total Environment. Elsevier B.V., http://dx.doi.org/10.1016/j.scitotenv.2019.134893.

Herman, A., Herman, A.P., 2012. Caffeine's mechanisms of action and its cosmetic use. Skin Pharmacol. Physiol. 26, 8–14. http://dx.doi.org/10.1159/000343174.

Iruretagoyena, D., Bikane, K., Sunny, N., Lu, H., Kazarian, S.G., Chadwick, D., Pini, R., Shah, N., 2020. Enhanced selective adsorption desulfurization on co2 and steam treated activated carbons: Equilibria and kinetics. Chem. Eng. J. 379, 122356. http://dx.doi.org/10.1016/j.cej.2019.122356.

Kleywegt, S., Payne, M., Raby, M., Filippi, D., Ng, C.F., Fletcher, T., 2019. The final discharge: Quantifying contaminants in embalming process effluents discharged to sewers in ontario, Canada. Environ. Pollut. 252, 1476–1482. http://dx.doi.org/10.1016/j.envpol.2019.06.036.

Kumar, R., Sarmah, A.K., Padhye, L.P., 2019. Fate of pharmaceuticals and personal care products in a wastewater treatment plant with parallel secondary wastewater treatment train. J. Environ. Manag. 233, 649–659. http://dx.doi.org/10.1016/j.jenvman.2018.12.062.

Lawrence, M.A.M., Davies, N.A., Edwards, P.A., Taylor, M.G., Simkiss, K., 2000. Can adsorption isotherms predict sediment bioavailability? Chemosphere 41, 1091–1100. http://dx.doi.org/10.1016/S0045-6535(99)00559-7.

Lee, H.J., Kim, K.Y., Hamm, S.Y., Kim, M.S., Kim, H.K., Oh, J.E., 2019. Occurrence and distribution of pharmaceutical and personal care products, artificial sweeteners, and pesticides in groundwater from an agricultural area in Korea. Sci. Total Environ. 659, 168–176. http://dx.doi.org/10.1016/j.scitotenv.2018.12.258.

Li, S., Wen, J., He, B., Wang, J., Hu, X., Liu, J., 2020. Occurrence of caffeine in the freshwater environment: Implications for ecopharmacovigilance. Environ. Pollut. 263, 114371. http://dx.doi.org/10.1016/j.envpol.2020.114371.

Li, J., Yu, G., Pan, L., Li, C., You, F., Xie, S., Wang, Y., Ma, J., Shang, X., 2018. Study of ciprofloxacin removal by biochar obtained from used tea leaves. J. Environ. Sci. (China) 73, 20–30. http://dx.doi.org/10.1016/j.jes.2017.12.024.

Li, X., Zhu, X., 2015. Tea: Types, production, and trade. Encycl. Food Heal. 279–282. http://dx.doi.org/10.1016/B978-0-12-384947-2.00684-X.

Liu, N., Liu, Y., Zeng, G., Gong, J., Tan, X., Wen, Jun, Liu, S., Jiang, L., Li, M., Yin, Z., 2020. Adsorption of 17$\beta$-estradiol from aqueous solution by raw and direct/pre/post-KOH treated lotus seedpod biochar. J. Environ. Sci. (China) 87, 10–23. http://dx.doi.org/10.1016/j.jes.2019.05.026.

Loos, R., Carvalho, R., António, D.C., Comero, S., Locoro, G., Tavazzi, S., Paracchini, B., Ghiani, M., Lettieri, T., Blaha, L., Jarosova, B., Voorspoels, S., Servaes, K., Haglund, P., Fick, J., Lindberg, R.H., Schwesig, D., Gawlik, B.M., 2013. EU-wide monitoring survey on emerging polar organic contaminants in wastewater treatment plant effluents. Water Res. 47, 6475–6487. http://dx.doi.org/10.1016/j.watres.2013.08.024.

Luo, Y., Guo, W., Ngo, H.H., Nghiem, L.D., Hai, F.I., Zhang, J., Liang, S., Wang, X.C., 2014. A review on the occurrence of micropollutants in the aquatic environment and their fate and removal during wastewater treatment. Sci. Total Environ. 473–474, 619–641. http://dx.doi.org/10.1016/j.scitotenv.2013.12.065.

Ma, L., Liu, Y., Zhang, J., Yang, Q., Li, G., Zhang, D., 2018. Impacts of irrigation water sources and geochemical conditions on vertical distribution of pharmaceutical and personal care products (PPCPs) in the vadose zone soils. Sci. Total Environ. 626, 1148–1156. http://dx.doi.org/10.1016/j.scitotenv.2018.01.168.

Manyà, J.J., 2012. Pyrolysis for biochar purposes: A review to establish current knowledge gaps and research needs. Environ. Sci. Technol. 46, 7939–7954. http://dx.doi.org/10.1021/es301029g.

Mayakaduwa, S.S., Herath, I., Ok, Y.S., Mohan, D., Vithanage, M., 2017. Insights into aqueous carbofuran removal by modified and non-modified rice husk biochars. Environ. Sci. Pollut. Res. 24, 22755–22763. http://dx.doi.org/10.1007/s11356-016-7430-6.

Mayakaduwa, S.S., Vithanage, M., Karunarathna, A., Mohan, D., Ok, Y.S., 2016. Interface interactions between insecticide carbofuran and tea waste biochars produced at different pyrolysis temperatures. Chem. Speciat. Bioavailab. 28, 110–118. http://dx.doi.org/10.1080/09542299.2016.1198928.

van der Merwe, F.O., 1988. Caffeine in sport-urinary excretion of caffeine in health volunteers after intake of common caffeine-containing beverages. S. Afr. Med. J. 74, 163–164.

Muter, O., Pērkons, I., Bartkevičs, V., 2019. Removal of pharmaceutical residues from wastewater by woodchip-derived biochar. Desalin. Water Treat. 159, 110–120. http://dx.doi.org/10.5004/dwt.2019.24108.

Odendaal, C., Seaman, M.T., Kemp, G., Patterton, H.E., Patterton, H.G., 2015. An LC-MS/MS based survey of contaminants of emerging concern in drinking water in South Africa. S. Afr. J. Sci. 111, 1–6. http://dx.doi.org/10.17159/sajs.2015/20140401.

Pang, X., Ran, X., Kuang, F., Xie, J., Hou, B., 2010. Inhibiting effect of ciprofloxacin, norfloxacin and ofloxacin on corrosion of mild steel in hydrochloric acid. Chin. J. Chem. Eng. 18, 337–345. http://dx.doi.org/10.1016/S1004-9541(08)60362-6.

Phan, H.V., Hai, F.I., McDonald, J.A., Khan, S.J., Zhang, R., Price, W.E., Broeckmann, A., Nghiem, L.D., 2015. Nutrient and trace organic contaminant removal from wastewater of a resort town: Comparison between a pilot and a full scale membrane bioreactor. Int. Biodeterior. Biodegrad. 102, 40–48. http://dx.doi.org/10.1016/j.ibiod.2015.02.010.

Picó, Y., Alvarez-Ruiz, R., Alfarhan, A.H., El-Sheikh, M.A., Alshahrani, H.O., Barceló, D., 2020. Pharmaceuticals, pesticides, personal care products and microplastics contamination assessment of al-hassa irrigation network (Saudi Arabia) and its shallow lakes. Sci. Total Environ. 701, 135021. http://dx.doi.org/10.1016/j.scitotenv.2019.135021.

Ptaszkowska-Koniarz, M., Goscianska, J., Pietrzak, R., 2018. Synthesis of carbon xerogels modified with amine groups and copper for efficient adsorption of caffeine. Chem. Eng. J. 345, 13–21. http://dx.doi.org/10.1016/j.cej.2018.03.132.

Rajapaksha, A.U., Vithanage, M., Ahmad, M., Seo, D.C., Cho, J.S., Lee, S.E., Lee, S.S., Ok, Y.S., 2015. Enhanced sulfamethazine removal by steam-activated invasive plant-derived biochar. J. Hazard. Mater. 290, 43–50. http://dx.doi.org/10.1016/j.jhazmat.2015.02.046.

Rajapaksha, A.U., Vithanage, M., Zhang, M., Ahmad, M., Mohan, D., Chang, S.X., Ok, Y.S., 2014. Pyrolysis condition affected sulfamethazine sorption by tea waste biochars. Bioresour. Technol. 166, 303–308. http://dx.doi.org/10.1016/j.biortech.2014.05.029.

Rybak, M.E., Sternberg, M.R., Pao, C.-I., Ahluwalia, N., Pfeiffer, C.M., 2015. Urine excretion of caffeine and select caffeine metabolites is common in the US population and associated with caffeine intake. J. Nutr. 145, 766–774. http://dx.doi.org/10.3945/jn.114.205476.

San Miguel, G., Fowler, G.D., Sollars, C.J., 2003. A study of the characteristics of activated carbons produced by steam and carbon dioxide activation of waste tyre rubber. Carbon N. Y. 41, 1009–1016. http://dx.doi.org/10.1016/S0008-6223(02)00449-9.

Seneviratne, M., Vithanage, M., Madawala, H.M.S.P., Seneviratne, G., 2015. A novel microbial biofilm for bioremoval of nickel from aqueous media. Bioremediat. J. 19, 239–248. http://dx.doi.org/10.1080/10889868.2014.995374.

Singh, B., Camps-Arbestain, M., Lehmann, J., CSIRO (Australia), 2017. Biochar: A Guide to Analytical Methods, Csiro Publishing. Csiro Publishing.

Solanki, A., Boyer, T.H., 2017. Pharmaceutical removal in synthetic human urine using biochar. Environ. Sci. Water Res. Technol. 3, 553–565. http://dx.doi.org/10.1039/c6ew00224b.

Sotelo, J.L., Ovejero, G., Rodríguez, A., Álvarez, S., Galán, J., García, J., 2014. Competitive adsorption studies of caffeine and diclofenac aqueous solutions by activated carbon. Chem. Eng. J. 240, 443–453. http://dx.doi.org/10.1016/j.cej.2013.11.094.

Sun, Y., Cho, D.W., Graham, N.J.D., Hou, D., Yip, A.C.K., Khan, E., Song, H., Li, Y., Tsang, D.C.W., 2019. Degradation of antibiotics by modified vacuum-UV based processes: Mechanistic consequences of H 2 O 2 and K 2 S 2 O 8 in the presence of halide ions. Sci. Total Environ. 664, 312–321. http://dx.doi.org/10.1016/j.scitotenv.2019.02.006.

Torrellas, S.Á., García Lovera, R., Escalona, N., Sepúlveda, C., Sotelo, J.L., García, J., 2015. Chemical-activated carbons from peach stones for the adsorption of emerging contaminants in aqueous solutions. Chem. Eng. J. 279, 788–798. http://dx.doi.org/10.1016/j.cej.2015.05.104.

Álvarez Torrellas, S., Rodríguez, A., Ovejero, G., Gómez, J.M., García, J., 2016. Removal of caffeine from pharmaceutical wastewater by adsorption: Influence of NOM, textural and chemical properties of the adsorbent. Environ. Technol. (U. K.) 37, 1618–1630. http://dx.doi.org/10.1080/09593330.2015.1122666.

Tran, H.N., You, S.J., Chao, H.P., 2017. Fast and efficient adsorption of methylene green 5 on activated carbon prepared from new chemical activation method. J. Environ. Manag. 188, 322–336. http://dx.doi.org/10.1016/j.jenvman.2016.12.003.

Uzun, B.B., Apaydin-Varol, E., Ateş, F., Özbay, N., Pütün, A.E., 2010. Synthetic fuel production from tea waste: Characterisation of bio-oil and bio-char. Fuel 89, 176–184. http://dx.doi.org/10.1016/j.fuel.2009.08.040.

Vithanage, M., Mayakaduwa, S.S., Herath, I., Ok, Y.S., Mohan, D., 2016. Kinetics, thermodynamics and mechanistic studies of carbofuran removal using biochars from tea waste and rice husks. Chemosphere 150, 781–789. http://dx.doi.org/10.1016/j.chemosphere.2015.11.002.

Xu, R., Zhang, P., Wang, Q., Wang, X., Yu, K., Xue, T., Wen, X., 2019. Influences of multi influent matrices on the retention of PPCPs by nanofiltration membranes. Sep. Purif. Technol. 212, 299–306. http://dx.doi.org/10.1016/j.seppur.2018.11.040.

Zhang, M., Ahmad, M., Al-Wabel, M.I., Vithanage, M., Rajapaksha, A.U., Kim, H.S., Lee, S.S., Ok, Y.S., 2015. Adsorptive removal of trichloroethylene in water by crop residue biochars pyrolyzed at contrasting temperatures: Continuous fixed-bed experiments. J. Chem. 2015, 1–6. http://dx.doi.org/10.1155/2015/647072.

Zhang, Y.J., Xing, Z.J., Duan, Z.K., Li, M., Wang, Y., 2014. Effects of steam activation on the pore structure and surface chemistry of activated carbon derived from bamboo waste. Appl. Surf. Sci. 315, 279–286. http://dx.doi.org/10.1016/j.apsusc.2014.07.126.